Three-dimensional imaging of director field orientations in liquid crystals by polarized four-wave mixing microscopy

Bi-Chang Chen and Sang-Hyun Lim[a)]
Department of Chemistry and Biochemistry, University of Texas at Austin, 1 University Station A5300, Austin, Texas 78712, USA

(Received 30 March 2009; accepted 13 April 2009; published online 30 April 2009)

We report that nondegenerate four-wave mixing (FWM) signals from liquid crystals (LCs) excited by near IR ultrafast pulses can probe local molecular orientations of LCs. The two laser pulses are selected out of a single broadband Ti:sapphire laser by a pulse shaper and focused on LC samples to generate strong FWM signals. We demonstrate laser-scanning FWM microscopy with topological defects in a smectic A LC material. The image contrast originates from the anisotropic nonlinear response of LC molecules and the high signal sensitivity allows fast depth-resolved imaging. © *2009 American Institute of Physics*. [DOI: 10.1063/1.3127535]

The long-range orientational order is one of the most important properties of liquid crystals (LCs).[1] Average molecular orientations of LC materials are described by the director field $\vec{n}(r)$, and noninvasive three-dimensional (3D) imaging of the director field structures is essential for fundamental studies and technological applications of LCs. Various confocal and nonlinear optical microscopy methods have been applied to LC studies for this purpose.[2–7] Fluorescence confocal polarizing microscopy can map out the 3D structures of LCs by measuring polarized fluorescence from anisotropic dyes doped in LC.[6] It requires special fluorescent dyes that align homogeneously with LC molecules. Label-free 3D optical imaging of LCs has been demonstrated by several nonlinear optical microscopy techniques. Third harmonic generation (THG) from LC molecules can provide 3D structural information but the interpretation of a THG image is complicated due to the interplay between the Gouy phase shift and the phase matching condition.[4] Three-photon fluorescence from LCs has also been used to study polymer-dispersed LCs.[7] Recently, coherent anti-Stokes Raman scattering (CARS) polarized microscopy has been applied to LC studies.[2,3,5] This method is label-free and can image the 3D structures of LCs with great sensitivity and also provide the information of molecular structures since it measures the polarized vibrational response of the sample molecules. It requires, however, a specialized laser system (two synchronized picosecond lasers) and its application to LC study is still limited to a few research groups.[2,3,5]

Here we demonstrate label-free 3D imaging of director field orientations in LC by nondegenerate four-wave mixing (FWM) microscopy. It requires a single broadband Ti:sapphire laser and directly visualizes 3D patterns of LC director fields with great sensitivity. FWM is a third order nonlinear optical process that generates signals at the frequency of $2\omega_1-\omega_2$ when the sample is excited by two laser pulses at the frequencies of ω_1 and ω_2. We select both ω_1 and ω_2 laser pulses from a single ultrafast laser utilizing a pulse shaper to generate strong FWM signals from LC samples. In THG, the effect of the Guoy phase shift which flips the optical phase of the laser pulses across the focal point of the laser pulse, cancels out THG signals in homogeneous samples.[4] This effect is greatly reduced in FWM since the frequencies of laser pulses (ω_1 and ω_2) and signals (~700 nm) are closer to each other and the phase mismatch is significantly canceled out.[8] Thus FWM generates much stronger signals than THG and it can be applied to optical microscopy without any symmetry restriction of the samples. In addition, thermotropic LC materials typically have large nonlinear responses due to their highly ordered molecular orientations and existence of conjugated backbone moieties such as the biphenyl group. Here we report that the FWM signals from LCs are highly polarized along the orientational direction of the LC chains and it provides a great contrast mechanism for 3D imaging of LC structures.

We select two laser pulses at 755 nm (ω_1, bandwidth ~20 nm) and 815 nm (ω_2, bandwidth ~40 nm) out of a single cavity-dumping oscillator laser pulse (~10 fs, 2 MHz, Cascade, KM laboratories) with an all reflective $4f$ pulse shaper based on a LC spatial light modulator (SLM-640, CRI) [Fig. 1(a)]. The spectra of the laser pulses and typical FWM signals from LCs are shown in Fig. 1(b). Detailed description of our pulse shaper can be found in our earlier publication.[9] The wavelengths of lasers shorter than 740 nm are blocked by a razor blade placed at the Fourier plane of the pulse shaper. Note that the two laser pulses (ω_1 and ω_2) are not spatially separated and follow the identical optical path. The shaped laser pulses are focused into the

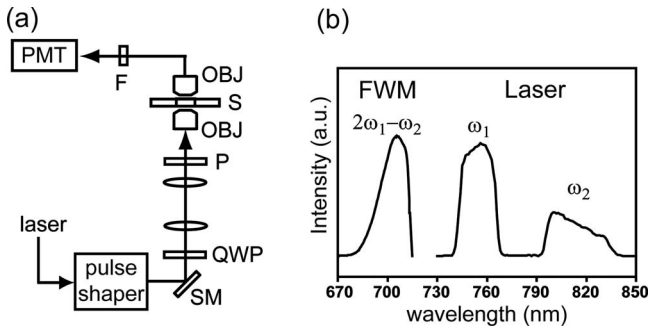

FIG. 1. (a) Experimental setup: SM, piezo beam-scanning mirror; QWP, quarter-wave plate; P, polarizer; OBJ, microscope objective; S, sample; F, short-wave pass filter; and PMT, photomultiplier tube. (b) Spectra of the shaped laser pulse and the FWM signal from 5CB. Note that intensities of the laser and the FWM signal are in different scales.

a)Electronic mail: shlim@mail.utexas.edu.

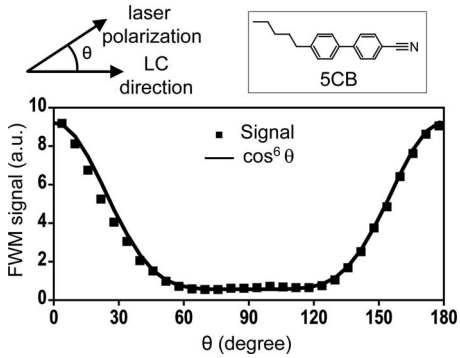

FIG. 2. Experimental FWM signal intensity vs the angle θ between the directions of the laser polarization and the chain orientation of an aligned 5CB film (molecular structure shown in the inset). The solid curve is the fit of $\cos^6\theta$ to the experimental data. Note that the polarization contrast is better than ten.

sample and FWM signals are collected with 1.2 and 1.0 numerical aperture (NA) objective lenses (Olympus), respectively. The collected signals are then filtered by a short wave pass filter (710 AESP, Omega Optical) and detected with a photomultiplier tube (PMT) (H5784–20, Hamamatsu). The laser beam is raster-scanned in the horizontal sample plane by a piezodriven scanning mirror (SM) [shown in Fig. 1(a), P-542.2SL, PI] to acquire depth-resolved images. The vertical position of the sample is controlled by a translational sample stage with a motorized actuator (Z606, Thorlabs). The polarization of the laser pulse is controlled by a combination of a quarter-wave plate (ACWP, CVI) and a polarizer (Versalight Polarizer, Meadowlark). We first convert the linearly polarized laser beam into a circularly polarized one and select the direction of linear polarization with the polarizer. The polarizer is mounted on a flipper mount such that circularly polarized laser can also be used to image the same area of the sample. The spectral phase (chirp) of the laser pulse at the sample position of the microscope is characterized by the homodyne spectral phase interferometry for direct electric field reconstruction technique (SPIDER) that we have developed recently.[10] Applying the compensating phase mask compresses the laser pulse at the focus of the microscope.

Figure 2 shows the polarization angle dependence of the FWM signals from an aligned nematic LC film [pentylcyanobiphenyl (5CB)] (Aldrich). A small amount of 5CB is sandwiched between two glass coverslips coated with a rubbed poly(vinyl alcohol) film to set a unidirectional LC alignment. A 50 μm thick mylar film is used as a spacer. The polarization of the laser pulse is changed by rotating the polarizer angle while adjusting the amplitude mask of SLM to keep the laser power identical at each polarization angle. The FWM signal intensity is highest when the polarization direction of the laser pulses is parallel to the molecular orientation of LC. One can clearly see the theoretically predicted $\cos^6\theta$ dependence of FWM signals, where θ is the angle between the directions of the laser polarization and the orientation of aligned 5CB molecules. The contrast from the polarization dependence of the FWM signals of LCs is better than ten, as shown in Fig. 2.

To demonstrate the 3D orientational imaging capability of our FWM microscopy, we choose the so-called focal conic domains (FCDs) formed in a smectic A phase of octylcyanobiphenyl (8CB) (Aldrich). FCD is a class of topological defects where parallel lamellar layers of LC molecules fold around a pair of confocal hyperbolic and elliptical defect lines located in the two mutually perpendicular planes.[2,3,6] Figure 3(a) shows the schematic director field structure of a FCD domain. Note that Fig. 3(a) shows only the lower half of the entire FCD domain. The lamellar layers of LC molecules are normal to the director field shown in Fig. 3(a).[2]

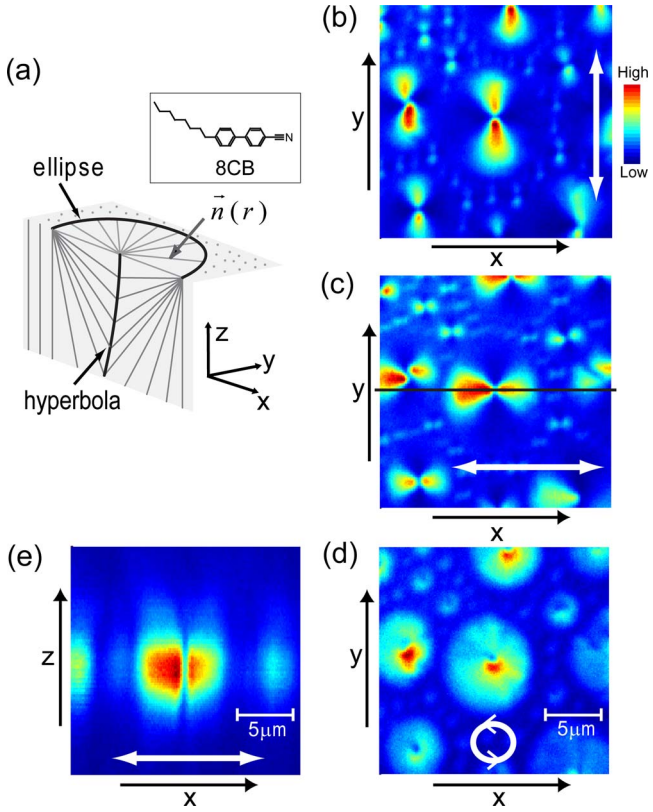

FIG. 3. (Color online) (a) 3D pattern of director fields, $\vec{n}(r)$ of a FCD in a smectic A LC. (Inset: the molecular structure of 8CB). Note that only the lower half of the FCD domain is shown. [(b)–(d)] Horizontally sectioned FWM images of FCDs in an 8CB film. The laser polarization direction is along Y and X axes in [(b) and (c)], respectively. Circularly polarized laser pulses are used in (d). (e) Vertical cross section along the black line in (c). White arrows represent the laser polarization directions in [(b)–(e)]. All the image sizes are 20×20 μm^2.

Figures 3(b)–3(e) shows the experimental FWM images of FCDs formed in an 8CB film at the room temperature. A small drop of 8CB is sandwiched between two clean glass coverslips with a 50 μm thick mylar film as a spacer. The FWM images are acquired by raster-scanning of the laser beam at the speed of 20 000 pixels/s (pixel dwell time is 50 μs/pixel). It takes 2 s to obtain a 200×200 pixels image with our current setup. The powers of the laser pulses at ω_1 and ω_2 are 0.4 and 0.2 mW, respectively. When one pulse is delayed ~100 fs by applying a linear spectral phase (i.e., time delay) in the SLM, FWM signals virtually disappear to confirm that the image contrast is not due to multiphoton fluorescence. When a different laser-blocking filter (BG28) that transmit UV signals, we do observe three-photon fluorescence signals around at 400 nm as Xie and Higgins[7] reported previously. However, the short wave pass filter used in our setup completely blocks UV fluorescence signals, and the image contrast in Fig. 3 is solely from FWM process.

Figures 3(b)–3(d) are in-plane XY sections of FCDs with three different laser polarizations. With linearly polarized la-

ser pulses, the strongest FWM signal is generated at the part of the sample where the local director fields are parallel to the laser polarization direction. When circularly polarized laser pulses are used, FWM probes the projection of the director fields onto the *XY* plane [Fig. 3(d)]. Thus one can get the information for vertical polarization components (i.e., *Z* polarization) of LC director fields from the circular polarization experiment if the sample has a uniform concentration distribution. In Fig. 3(d), the low signal region is where the LC director fields are oriented along the *Z* axis and the high signal area is where the director fields are parallel to the *XY* plane. One can see the elliptical defect lines of FCDs in Fig. 3(d). Figures 3(b)–3(d) clearly show that one can map out the orientation of the local director fields at a horizontally sectioned plane of the LC sample. Figure 3(e) is the vertically sectioned FWM image along the black cut line in Fig. 3(c). The laser polarization direction is parallel to the *X* axis. The hyperbola defect line is clearly visible in Fig. 3(e) demonstrating the depth-resolving capability of FWM microscopy.

It is well known that a high power laser pulse can realign the orientation of LC molecules.[3] This optical Fredericks effect has been observed in much higher laser powers (>100 mW) in the previous reports.[3,5] In the current work, we use the total laser power of ~0.6 mW and the laser-induced realignment effect has not been observed. The excellent contrast of the images in Fig. 3 is due to the high signal level generated by very short laser pulses (~60 and ~40 fs for ω_1 and ω_2, respectively) and their strong polarization angle dependence. Note that the image contrast comes from the distributions of molecular orientations, not those of the concentration gradients of LCs since the sample has only a single LC species. With the total laser power of 1 mW, the FWM signal from 8CB sample can easily saturate our PMT at a moderate gain with 50 μs exposure time. The current limitation of the imaging speed is due to the use of the piezo beam-steering mirror and it is straightforward to upgrade the setup with a faster galvo scanner.

Most of the detected FWM signals originate from the nonlinear electronic response of LCs. Since the electronic nonlinear response is highly anisotropic due to the strong orientational order of LC molecules, we can obtain high contrast FWM images. However, there is some contribution from nonlinear vibrational response, i.e., CARS.[9] The two laser pulses (ω_1 and ω_2) can create coherent vibrational motions of LC molecules and ω_1 pulse can scatter the vibrational excitations nonelastically to generate CARS signals at the same frequency range of our FWM signals. We verified the amount of vibrational contribution by applying a narrow π-shifted phase mask at the center of the ω_1 pulse.[9] If the signal spectrum with the π-shifted phase mask is measured, this experiment becomes the interferometric multiplex CARS spectroscopy we have developed recently.[9] We estimate that the vibrational contribution is less than 1% of the total detected signals from the interference modulation depth of the measured multiplex CARS spectrum.[9] In fact, the electronic FWM signal is equivalent to the so-called nonresonant background in CARS experiments.[11] Upon the excitation by short femtosecond laser pulses, the nonresonant CARS signals can be many orders of magnitude larger than the vibrational CARS signal.[9,11] What we demonstrate here is that the nonresonant background can be used for orientational imaging of LCs. We have previously demonstrated a spectral interferometric CARS method, which can extract the background-free vibrational spectrum of a sample against the nonresonant background.[9] It is easy to implement both FWM and multiplex CARS microspectroscopy in a single experimental setup and we expect that the combination of these two imaging modalities will be a powerful tool for studies of complex LC systems.

In this work, we use a pulse shaper to select two laser pulses (ω_1 and ω_2 pulses) and compress them at the sample position of the microscope. However, one can also perform 3D imaging of LCs without a pulse shaper if the bandwidth of the laser is broad enough to generate FWM signals at the frequency range where one can detect after blocking the laser pulse. In this case, there is a significant region of the laser frequencies that does not contribute detectable signals and the pulse compression by prism or grating pairs is not as perfect as in our experiment. However, the signal level we observe in this work suggests that it will be likely to obtain high contrast images by the simpler experimental setup.

In summary, we demonstrate that nondegenerate electronic FWM process can be used for noninvasive label-free 3D imaging of LCs. It produces a high quality image within a couple of seconds and an upgrade to a faster acquisition speed is straightforward. Combination of linear and circular laser polarization allows one to study the 3D orientational structures of LC director field in detail. The strong signal level can afford a faster imaging speed and it might be able to study dynamic phenomena of LC materials.

The authors gratefully acknowledge the Welch Foundation for support of personnel (Project F-1663).

[1] P. G. de Gennes and J. Prost, *The Physics of Liquid Crystals* (Clarendon, Oxford, 1993).
[2] A. V. Kachynski, A. N. Kuzmin, P. N. Prasad, and I. I. Smalyukh, Appl. Phys. Lett. **91**, 151905 (2007).
[3] A. V. Kachynski, A. N. Kuzmin, P. N. Prasad, and I. I. Smalyukh, Opt. Express **16**, 10617 (2008).
[4] R. S. Pillai, M. Oh-e, H. Yokoyama, G. J. Brakenhoff, and M. Muller, Opt. Express **14**, 12976 (2006); D. Yelin, Y. Silberberg, Y. Barad, and J. S. Patel, Appl. Phys. Lett. **74**, 3107 (1999).
[5] B. G. Saar, H.-S. Park, X. S. Xie, and O. D. Lavrentovich, Opt. Express **15**, 13585 (2007).
[6] I. I. Smalyukh, S. V. Shiyanovskii, and O. D. Lavrentovich, Chem. Phys. Lett. **336**, 88 (2001).
[7] A. Xie and D. A. Higgins, Appl. Phys. Lett. **84**, 4014 (2004).
[8] J.-X. Cheng, A. Volkmer, and X. S. Xie, J. Opt. Soc. Am. B **19**, 1363 (2002).
[9] B.-C. Chen and S.-H. Lim, J. Phys. Chem. B **112**, 3653 (2008).
[10] J. Sung, B.-C. Chen, and S.-H. Lim, Opt. Lett. **33**, 1404 (2008).
[11] J.-X. Cheng and X. S. Xie, J. Phys. Chem. B **108**, 827 (2004).